Radiography Open

ISSN: 2387-3345 Vol 8, No 1 (2022) https://doi.org/10.7577/radopen.5004

Could posterior-anterior projection cervical spine radiographs improve image quality and dose reduction

R. Faulkner[1], P. Lockwood*[2]

[1] Radiology Department, Bristol Royal Infirmary, University Hospitals Bristol and Weston NHS Foundation Trust, Bristol, United Kingdom.

[2]School of Allied Health Professions, Faculty of Medicine, Health and Social Care, Canterbury Christ Church University, Kent, United Kingdom.

*Corresponding author e-mail address: paul.lockwood@canterbury.ac.uk

Keywords: Cervical Spine; Image Quality; Radiation Dose; Scatter radiation, Phantom study

Abstract

Introduction: Anterior-posterior (AP) cervical spine X-rays are routine examinations to assess degenerative change, persistent pain and traumatic injuries. Multiple radiosensitive organs lie anteriorly within this anatomical region, increasing the stochastic risk of cancer. If a posterior-anterior (PA) projection was utilised, the radiation dose could potentially be reduced. The hypothesis of this study is to evaluate the change in radiation dose and image quality between AP and PA positions.

Materials and methods: An anthropomorphic phantom was positioned AP erect against a digital radiography (DR) detector with 30 thermoluminescent dosimeters (TLDs) inserted to record the thyroid, breast, ovaries, and testes absorbed radiation dose at an exposure of 66 kV and 8 mAs. The phantom was repositioned PA erect and repeated. Images were assessed against an image quality criteria Likert scale by qualified radiographers. The mean and standard deviations were calculated for dose and image quality and compared using a *t*-test and Wilcoxon Signed Ranks Test.

Results: The PA erect cervical spine reduced radiation dose to the right thyroid by 92% (44.7 µGy; p=0.00) and the left thyroid by 89% (43.7 µGy; p=0.00), with further reductions in

scatter dose to the breasts (0.35-0.45 µGy; *p*=0.85), ovaries (0.41 µGy; *p*=0.57), and testes (0.04 µGy; *p*=0.98). Image quality scores for the end plates, pedicles, joint spaces, spinous and transverse processes, cortical and trabecular bone patterns, and soft tissues were near equivalent (*p*=0.32).

Conclusion: Data analysis suggests that PA cervical spine positioning for X-rays in the laboratory adheres to as low as reasonably practicable (ALARP) guidance on X-ray examinations to reduce radiation dose to male and female internal organs (thyroid, breast, ovaries) without a reduction in image quality compared to AP positioning. Further research in clinical practice is advised.

Introduction

Between 2020-2021, 16.8 million plain film X-rays were performed in England, making it the most popular imaging modality within radiology.[1] Cervical spine X-rays are commonly requested to assess degenerative changes, persistent neck pain and trauma injuries. This examination requires the patient to be in the anterior-posterior (AP) position and is routinely accompanied by a lateral view and an odontoid peg view for trauma.[2]

The challenge with AP cervical spine views is that radiosensitive organs such as the breast, ovaries and testes[3] lie anterior in the body and are susceptible to scattered secondary radiation increasing the stochastic risk of developing cancer.[4] As such, radiographers must adhere to keeping radiation dose 'as low as reasonably practicable' (ALARP).[5,6] Although it is accepted that radiation doses for cervical spine anatomy and the surrounding organs receiving scattered radiation are low, small changes to imaging parameters and positioning can assist in reducing doses for patients receiving repeated follow-up x-ray examinations for degenerative changes. However, Image quality is equally important in identifying fractures and pathology, and underexposed images can result in misdiagnosis.[7]

In clinical practice, the AP projection is recommended[8] as the vertebral column is located on the posterior aspect of the body, thus reducing the magnification of the anatomy to the image receptor.[9] If a PA projection[10] is used, a minor air gap magnification due to the anterior surface of the mandible being in contact with the image plate results in the cervical spine being a small distance from the surface of the image plate, which may affect the image quality. However, an air gap magnification can increase image contrast resolution by reducing a minor amount of secondary scatter radiation to the image plate. Furthermore, the cervical spine has minimal soft tissue structures lying anteriorly[11,12] to attenuate the X-ray beam, and the lordotic concavity of the curvature of the cervical vertebrae[11] follows the X-ray beam direction from the focal spot and reduces the superimposition of vertebral endplates on the image.[8,13]

A study by Davey and England[9] on PA lumbar spine X-ray examinations demonstrated that radiation dose could be reduced by X-ray photon attenuation from the body before reaching anteriorly positioned sensitive organs. This raises the possibility of PA cervical spine

examinations potentially reducing the dose for non-trauma examinations (PA views would be difficult for trauma patients triaged with stiff plastic neck collars/braces and immobilisation to spinal boards). Therefore, the aim of the study was to evaluate if routine (non-trauma) cervical spine X-ray examinations could be completed in the PA position to reduce patient dose whilst maintaining or improving image quality. The null hypothesis (H_0) was no change in image quality or dose. The alternative hypothesis (H_1) was the image quality would change, but the dose would remain constant. The second alternative hypothesis (H_2) was the dose would change, but the image quality would remain constant.

Methods

Institutional ethical approval (ETH2122-S19/RPR/01) was granted for the study (exposures within a controlled X-ray laboratory and participant image evaluation), and local rules were followed according to Ionizing Radiation Regulations.[14] The X-ray tube (Siemens Opti X-ray unit 150/30/50HC-100, Germany) was quality assured to obtain consistent X-ray output. To achieve this, an ion chamber (Fluke Biomedical LCC TNT 12000 system, United States) was positioned upon a tissue equivalent block connected to a test meter (Fluke Biomedical LCC DoseMate, United States) and dose area product meter (DAP) (KermaX plus iba Dosimetry, Belgium). The exposure factors of 66 Kilovoltage (kV) and 8 Milliamperes second (mAs) were used with a source-to-image distance (SID) of 100 centimetres (cm).[2] Five exposures were completed, and DAP and ion chamber readings were recorded (figure. 1).

Figure 1. The ion chamber is positioned upon a tissue equivalent block to quality assure the X-ray tube output.

Before the experiment, *n*=30 thermoluminescent dosimeters (TLDs; Landauer, TLD-100H, England) were annealed in a Carbolite TLD oven (Carbolite Gero, England) to remove accumulated background radiation. The TLDs were made of Lithium Fluoride (LiF) crystals,[15] which were tissue equivalent (Human tissue Z = 7.4, LiF Z = 8.228). The manufacturing process causes microscopic crystal lattice imperfections and impurities[16] which act as electron traps to capture the X-ray energy when irradiated. Thus, each TLD has minor variations and can have an overestimation of dose up to 10-30%[17,18] if not calibrated to the

exposure factors used in the experiment beforehand.[17] Following the annealing process, the TLDs were placed upon the tissue equivalent block and exposed using the same exposure factors for the sensitivity calibration (figure. 2). These were placed into the TLD platen using vacuum tweezers (Dymax 30, Charles Austin Pumps Ltd, England) and placed into the TLD reader (Hawshaw 5500, Thermo Scientific, USA) to record the light count readings. Within this batch of *n*=30 TLDs variance of the sensitivity (due to manufacturing) difference was 3% after calibration.

Figure 2. The TLDs are positioned upon a tissue equivalent block to calibrate the sensitivity.

The readings were recorded, and the TLDs were grouped into sensitivity order and divided into nine labelled zip lock bags (*n*=3 TLDs per bag) to measure the background dose (most sensitive TLDs) and radiosensitive organs of the thyroid, breast, ovaries, and testes[19] (similar TLD sensitivities), the *n*=3 lowest sensitivity TLDs were removed from the batch as spares. An anthropomorphic phantom (Rando phantom, Alderson Research Laboratories Inc., United States) was positioned in the AP erect position against a digital radiography (DR) detector (AGFA NX3.0 Workstation, DXD 40C, Belgium). The TLD bags were placed into the transected-horizontal phantom slices at the right and left thyroid (slice 9), right and left breast (slice 16), right and left ovaries (slice 28), and right and left testes (slice 33, figure 3). The X-ray tube was set at 100cm SID and centred mid-neck soft tissue region (the fourth cervical vertebrae) as per standard clinical practice.[8] Collimation was set at 20cm x 20cm collimating laterally to the soft tissue margins of the neck, and top to the mandible and bottom to the cervical, thoracic junction,[8] so that the breast, ovaries and testes did not receive the primary x-ray beam. A 30-degree cranial angulation was incorporated for the AP position due to the fixed phantom mandible (Figure.3). The exposure factors of 66 kV and 8 mAs were used, and three rounds of exposures and TLD readings were accomplished to compensate for electricity fluctuation.

Figure 3. The phantom in AP position with the TLDs and X-ray tube 30-degree cranial angulation.

The TLDs were read between each exposure, and the results were recorded on a Microsoft Excel (United States, 2022) spreadsheet. The process to calculate the absorbed radiation dose from the TLD light count involved deducting the background radiation light counts from the anatomical placed TLD light count,[16] then using the Element Correction Coefficient (ECC),[17] Reader Calibration Factor (RCF),[17] and the final light count to dose unit Conversion Factor.[17]

Figure 4. The phantom positioned in PA with the TLDs and X-ray tube 30-degree caudal angulation.

The phantom was repositioned in the PA position[10] with annealed TLDs in the same anatomical slices (figure. 4). The X-ray tube was angled 30 degrees caudal to compensate for the fixed phantom head and neck position and centred mid-neck soft tissue region. The PA projection air gap magnification was calculated using the formula of SID (100cm) /source-object distance (88cm), resulting in an air gap magnification of 12cm between the anterior surface of the neck and the image plate to dissipate scatter radiation. The parameters maintained the 66 kV, 8 mAs, and collimation at 20cm x 20cm (lateral collimation to the

neck soft tissue margins, and top to the mandible and bottom to the cervical thoracic junction[8]) for three more exposures with the TLDs read between each exposure.

The TLD data analysis calculated a mean (interval data) dose for each radiosensitive organ's AP and PA positions. To determine the radiation dose (measuring the difference between the pairs of TLD interval data), a non-parametric statistical analysis using matched pairs *t*-Test to gain a *p*-value ($p \leq 0.05$) was applied.

All the examination images were saved onto the university picture archiving and communication system (PACS; IQ-Web; Image Information Systems, Germany). Three diagnostic radiography lecturers at the university with over ten years of clinical reporting experience were recruited to assess three AP and three PA images for image quality. All image assessors reviewed all six images, and all images were unidentified as to AP or PA position to reduce bias in observations and numbered. All the image assessors provided written consent before participating in the study. The images were assessed against the Image Quality Scoring (IQS) criteria from the European Commission[20] (table 1). The Likert ordinal scale used to grade the images against the individual level items (table 1) used a 1-5 scale of poor (1), acceptable (2), good (3), very good (4) and excellent (5). A subscale analysis of the item-by-item scores for each image and a median value (ordinal data) were calculated to compare the image quality of the AP and PA images.[5] To determine the diagnostic image quality hypothesis and measure the difference between the AP and PA IQS data, a non-parametric statistical analysis applied the Wilcoxon Matched Pairs Signed Ranks Test to gain a *p*-value ($p \leq 0.05$).[21] Wilcoxon Signed Rank Test is similar to the *t*-Test for matched pairs but is used for Likert ordinal scale values.

Table 1. The Image Quality Scoring (IQS) criteria.

1.1.1.	Visually sharp reproduction, as a single line, of the upper and lower-plate surfaces in centered beam area
1.1.2.	Visually sharp reproduction of the pedicles
1.1.3.	Reproduction of the intervertebral joints
1.1.4.	Reproduction of the spinous and transverse processes
1.1.5.	Visually sharp reproduction of the cortex and trabecular structures
1.1.6.	Reproduction of the adjacent soft tissues

Results

The mean PA dose to the radiosensitive organs compared to the AP dose was measured in micro milligray (µGy), demonstrating a significant reduction from the primary X-ray beam to the right thyroid of 92% (44.74 µGy; p=0.00) and the left thyroid by 89% (43.73 µGy; p=0.00) displayed in table 2. The *t*-test *p*-value for the primary beam organ dose was calculated to be below the 0.05 significance threshold rejecting the H_0. The PA secondary scatter radiation dose data also revealed a reduction (although not statistically significant due to the low scatter radiation measurements) in dose to the left breast (37%), right breast (31%)

and right ovary (39%) in table 2. A minor increase in scattered secondary radiation was demonstrated in the left ovary (0.02 µGy; *p*=0.23) and right testes (0.08 µGy; *p*=0.45; figure 5), potentially due to internal scatter[22] and noise at low dose measurement levels, and the sensitivity of TLDs at low doses.[16]

Table 2. The TLD dose data were recorded from the AP and PA positions.

		Anterior Posterior Projection (µGy)					Posterior Anterior Projection (µGy)					Dose Difference		*t*-test		
Beam	Anatomy	Exposure 1	Exposure 2	Exposure 3	Mean	SD	Exposure 1	Exposure 2	Exposure 3	Mean	SD	µGy	%	*t*-value	SD	*p*-value
Primary	Left Thyroid	46.59	50.33	51.03	49.32	2.39	5.88	5.7	5.19	5.59	0.36	-43.73	-88.7%	-35.03	2.13	*p*=0.00
Primary	Right Thyroid	51.52	46.1	47.59	48.4	2.80	2.55	3.22	5.21	3.66	1.38	-44.74	-92.4%	-21.12	3.67	*p*=0.00
Scatter	Left Breast	0.58	2.24	0.03	0.95	1.15	0.02	1.76	0.03	0.6	1.00	-0.35	-36.8%	-1.98	0.30	*p*=0.19
Scatter	Right Breast	4.07	0.01	0.09	1.39	2.32	0.07	0.02	2.79	0.96	1.59	-0.45	-30.9%	-0.22	3.37	*p*=0.85
Scatter	Left Ovary	0.02	0.03	0.04	0.03	0.01	0.02	0.07	0.06	0.05	0.03	0.02	66.6%	1.73	0.02	*p*=0.23
Scatter	Right Ovary	3.13	0.02	0.03	1.06	1.79	1.52	0.39	0.05	0.65	0.77	-0.41	-38.7%	-0.66	1.06	*p*=0.57
Scatter	Left Testes	3.65	0.02	0.02	1.23	2.10	0.59	2.97	0.01	1.19	1.57	-0.04	-3.3%	-0.02	3.01	*p*=0.98
Scatter	Right Testes	0.02	0.02	0.04	0.03	0.01	0.02	0.01	0.3	0.11	0.16	0.08	266.7%	0.94	0.15	*p*=0.45

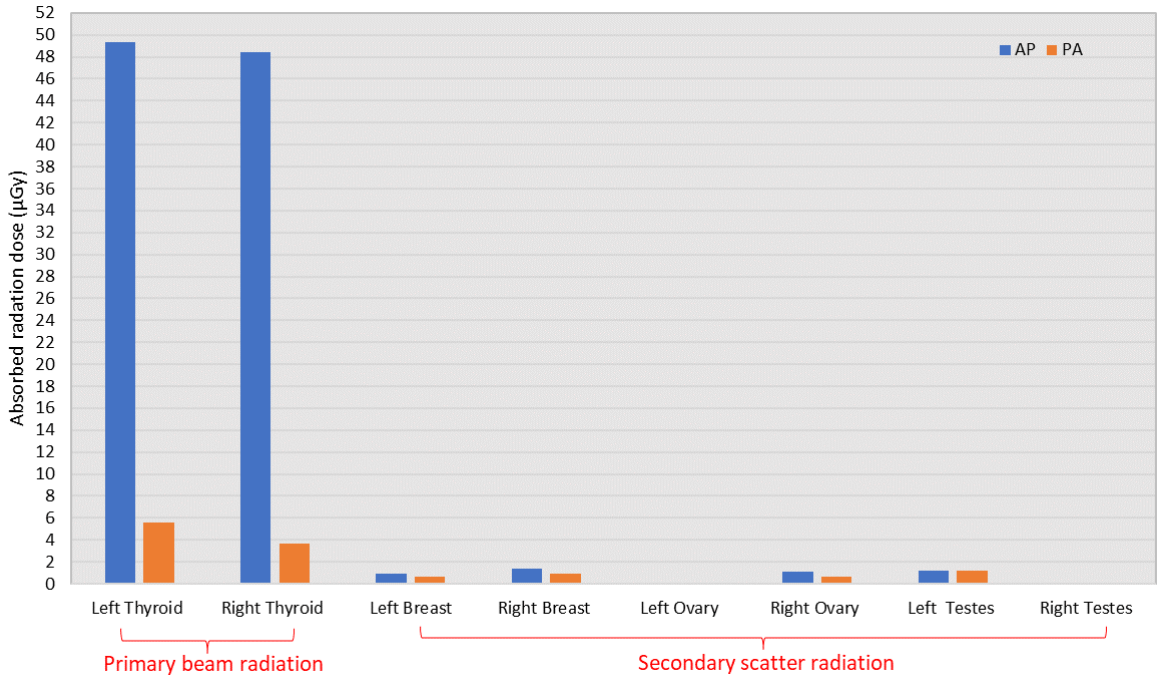

Figure 5. The reduction in mean absorbed radiation dose (µGy) between the AP and PA position by anatomical region measured

The AP and PA images acquired during the exposures (figures 6 and 7) of the phantom cervical spine anatomy displayed slight malalignment of the trachea and spinous processes due to the positioning of the phantom.

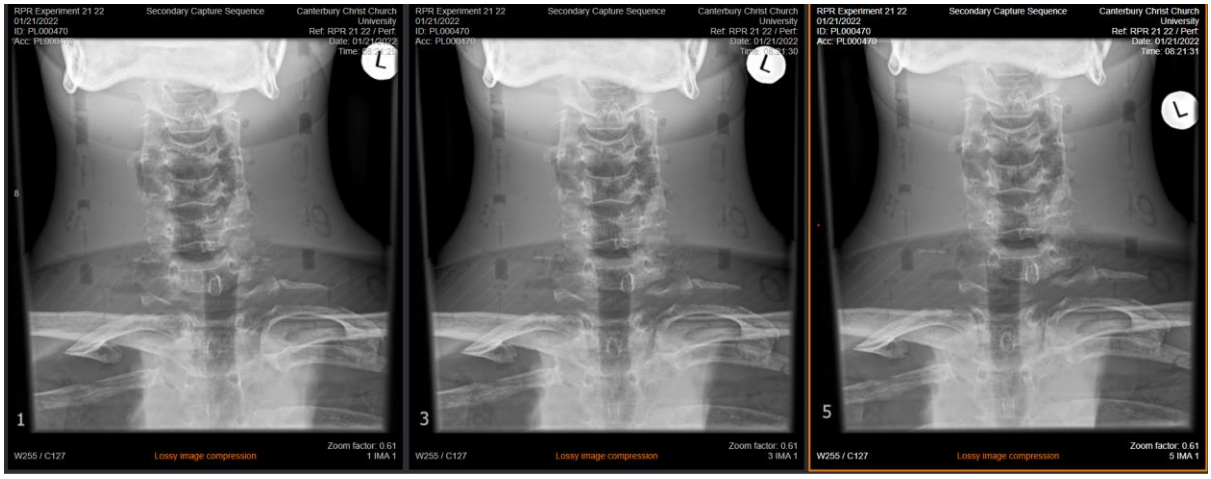

Figure 6. Three AP position phantom images were recorded to PACS for the IQS analysis.

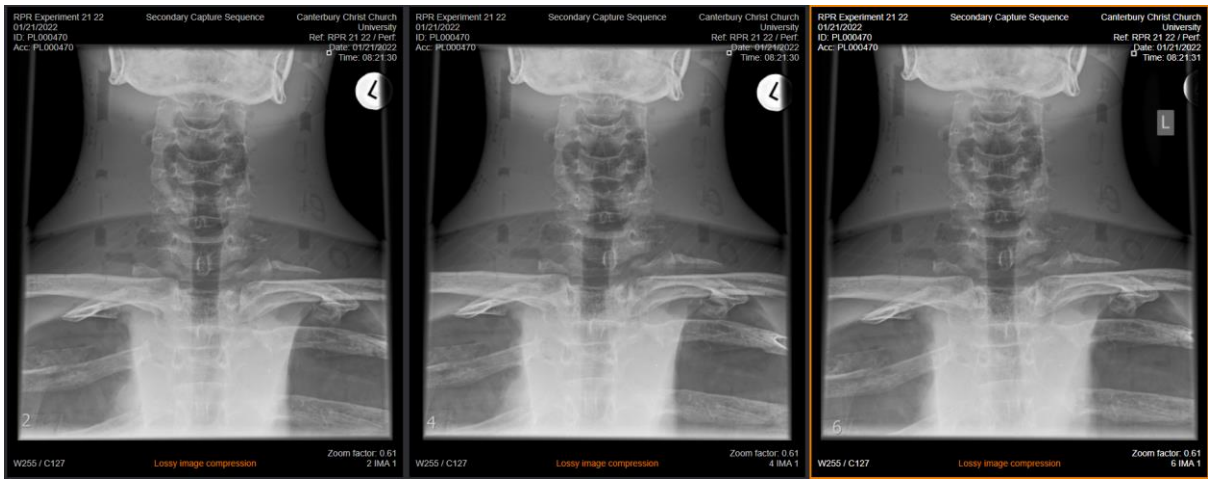

Figure 7. Three PA position phantom images were recorded to PACS for the IQS analysis.

The median IQS values for each image as assessed by the radiographer participants, along with the Wilcoxon Signed Rank *p*-values, are shown in table 3.

Table 3. Three radiographers reviewed the IQS data from the assessment of a random selection of three AP and PA positions phantom images.

Image Quality Criteria	AP C-Spine 1 Median IQS	AP C-Spine 2 Median IQS	AP C-Spine 3 Median IQS	PA C-Spine 1 Median IQS	PA C-Spine 2 Median IQS	PA C-Spine 3 Median IQS	Wilcoxon Signed Rank test *p*-value	Wilcoxon Signed Rank test *z*-value
1.1.1. Visually sharp reproduction, as a single line, of the upper and lower-plate surfaces in the centred beam area	9	6	7	10	9	8	*p*=0.1735	*z*=-1.3608
1.1.2. Visually sharp reproduction of the pedicles	8	8	6	7	5	9	*p*=1.0000	*z*=0.0000
1.1.3. Reproduction of the intervertebral joints	7	7	7	10	5	9	*p*=0.5862	*z*=-0.5443
1.1.4. Reproduction of the spinous and transverse processes	6	6	7	9	7	9	*p*=0.0946	*z*=-1.6712
1.1.5. Visually sharp reproduction of the cortex and trabecular structures	8	7	7	8	6	8	*p*=0.6373	*z*=-0.4714
1.1.6. Reproduction of the adjacent soft tissues	10	8	9	10	8	9	*p*=2.0000	*z*=0.5000
Aggregated Median	16	14	14.3	18	13.3	17.3	*p*=0.1112	*z*=-1.5927

The results show the statistically insignificant overall difference between the AP and PA IQS scores. A minor deviation in quality was shown in the upper and lower vertebral end plates in the AP position due to distortion caused by the tube angulation resulting from the fixed phantom position, which was statistically insignificant (IQS 1.1.1., table 3). Improved visualisation of the pedicles was recorded in the AP images, whilst the intervertebral joint space scores were slightly higher in the PA images (table 3). Reproduction of the cortex, trabeculae pattern and soft tissue appeared equal across all images.

The Wilcoxon *p*-value results were not statistically significant ($p > 0.05$), demonstrating that the AP image quality (figure 6) was equivalent to the PA images (figure 7). Thus, the overall outcome of the study results would reject H_0 and accept the H_2 that dose decreased from the AP to the PA position with equitable resulting image quality.

Discussion

Thyroid tissue is highly susceptible to ionizing radiation; the higher the dose, the higher the stochastic risks.[23] In the AP position, the thyroid is superficial to the skin surface and directly aligned to the collimated primary X-ray beam,[24] absorbing the highest radiation with minimal attenuation.[25] This study's results demonstrate that the PA position can significantly reduce thyroid dose by 89-92% ($p=0.00$; table 2) using the spine to attenuate the primary x-ray beam. Reducing patient doses contributes to a safer, more effective level of service for patients.[26]

Stephenson-Smith, Neep and Rowntree[27] in a study of $n=1,193$ reject X-rays (10.3%) from a collection of $n=11,596$ X-rays over a 3-month range from one X-ray room, suggest that positional errors were the main cause (58%) leading to repeated X-rays and additional patient radiation dose. If the patient's mandible is not sufficiently raised for AP cervical spine examinations, the mandible and occipital bones will superimpose over the cervical vertebra, resulting in repeat X-rays,[8] with the thyroid accumulating double the absorbed radiation dose and increasing the stochastic risk. The results in this study demonstrate that the risk in repeat imaging, if required, could be reduced if using PA positioning. It is expected that positioning patients for PA cervical spines would not require additional training as it carries a similar skill level to PA facial bones.[8]

The study maintained tight collimation to reduce scattered secondary radiation and improve image quality.[28] The inferior TLDs (breast, ovaries and testes) received a dose considerably less outside the collimated primary X-ray beam, similar to a shoulder X-ray study by Singh, Muscroft, Collier, and England[29] of tight collimation to reduce the dose to surrounding sensitive organs. A slight increase in dose was recorded in the left ovaries and right testes in the PA position (table 2), which was unexpected although insignificant. It is speculated these TLDs could have absorbed backscatter from the detector[10] or increased internal scatter.[22]

This increase was minimal, and a general reduction was demonstrated outside the collimated field (figure 5), although it is acknowledged that scattered doses are low.[22]

The PA position reduction in dose to radiosensitive organs correlates with Green, Karnati, Thomson, and Subramanian[25] study of PA lumbar spines, where the dose was reduced by 41% compared to AP positioning, and Ben-Shlomo et al.[3] theorised Monte-Carlo simulations of PA cervical, thoracic, and lumbar spine X-ray examinations. Additionally, the air gap of 12cm[30] may have assisted in reducing scatter radiation and improving image contrast resolution without affecting spatial resolution or image sharpness. However, cervical spine X-rays are recommended for trauma scenarios to be conducted AP with the patient supine on a trolley due to spinal immobilisation.[31] In this scenario, the PA cervical spine would be inappropriate,[32] and the PA cervical spine examination is recommended only for mobile non-trauma patients.

When analysing the image quality (table 3), the results showed a statistically insignificant overall change between the AP and PA images. These findings are similar to Davey and England's[9] phantom-based study of PA lumbar spines of diagnostically acceptable images. However, the lumbar spine has greater lordotic curvature but is comparable to the cervical spine images in our study. The main difference was due to the air gap magnification when the phantom was positioned in the PA projection; the object-to-image plate distance (12cm) due to the fixed mandible resulted in less sharpness of the pedicles[33,34] although this was a statistically insignificant image quality reduction (IQS 1.1.2, table 3).

Limitations of this study acknowledge the phantom used for dose measurements had a fixed position (inability to raise the mandible), requiring the X-ray tube angulation to be increased from 15 degrees cranial angulation in the AP[8] to 30 degrees cranial angulation. The PA position[10] required an angled 30-degree caudal to compensate for the fixed phantom model and superimpose the mandible and occipital bone.[8] The increase in angulation impacted the AP view and added minor distortion to the vertebral end plates and vertebral joint space[35] quality but was statistically insignificant (table 3). It is essential joint spaces are clearly defined as this can mimic dislocations[36] and is important for the degenerative diagnosis of joint spaces. The PA images resulted in a minor loss of sharpness of the pedicles,[33,34] although this was a statistically insignificant image quality reduction (table 3). However, less angulation would be needed in practice if the patient could effectively raise their mandible and the cervical spine had greater lordotic curvature than the rigid phantom, resulting in improved image quality. Likewise, it is acknowledged that adjustments to collimation and exposure parameters adjusted to the individual patient size in clinical practice will also lower the dose received in both views.

Conclusion

The study demonstrated a statistically significant reduction in radiation doses (89-92%; *p*=0.00) to the internal radiosensitive thyroid in the PA erect position compared to a standard AP erect projection within the primary X-ray beam for routine non-trauma cervical

spine examinations. The majority of secondary scattered radiation doses to the male and female internal radiosensitive organs and tissues in the PA erect position were lower than the standard AP erect projection. However, a statistically insignificant increase in the left ovary (0.02 µGy; p=0.23) and right testes (0.08 µGy; p=0.45) was recorded due to the sensitivity of TLDs, internal scatter, and noise at low dose measurement levels.

The cortex, trabeculae pattern and soft tissue reproduction in the image quality between the AP and PA positions demonstrated no statistically significant difference in IQS scores (p> 0.05). The negligible difference in quality was due to the fixed phantom positions (the AP position affected the upper and lower vertebral endplates but highlighted the pedicles; the PA position highlighted the intervertebral joint spaces).

The results align with clinical practice ALARP principles to reduce stochastic radiation risk. Further research in clinical practice is recommended to assess different X-ray equipment manufacturer doses and image quality on a range of different patient groups for clinical images. As well as a range of image reporters to assess IQS output to further verify the PA positioning technique.

References

1. NHS England. Diagnostic Imaging Dataset Annual Statistical Release 2019/2020. *Diagnostic Imaging Dataset Annual Statistical Release 2019/2020*. Available from: https://www.england.nhs.uk/statistics/wp-content/uploads/sites/2/2020/10/Annual-Statistical-Release-2019-20-PDF-1.4MB.pdf [accessed October 4, 2022].
2. Murphy A. Cervical Spine (AP View). *Radiopaedia*. Available from: https://radiopaedia.org/articles/cervical-spine-ap-view?lang=gb [accessed October 4, 2022].
3. Ben-Shlomo A., Bartal G., Mosseri M., Avraham B., Leitner Y., Shabat S. Effective dose reduction in spine radiographic imaging by choosing the less radiation-sensitive side of the body. *The Spine Journal* 2016;**16**(4):558–63. Doi: 10.1016/j.spinee.2015.12.012.
4. Cancer Research UK. Cancer Statistics for the UK. *Cancer Statistics for the UK*. Available from: https://www.cancerresearchuk.org/health-professional/cancer-statistics-for-the-uk [accessed October 4, 2022].
5. Chan CTP., Fung KKL. Dose optimization in pelvic radiography by air gap method on CR and DR systems – A phantom study. *Radiography* 2015;**21**(3):214–23. Doi: 10.1016/j.radi.2014.11.005.
6. UK Government. *Ionising Radiation (Medical Exposure) Regulations (IR(ME)R) 2017 (SI 2017/1322)*, London: HMSO; 2017.
7. Majeed A., Kanwal A., Naz N. Diagnostic Accuracy of Plain X-ray in Diagnosis of Cervical Spine Fracture, Keeping CT as Gold Standard. *Institute of Medical Science* 2016;**12**(3):171–4.
8. Whitley S., Sloane C., Jefferson G., Holmes K., Anderson C. *Clarke's Pocket Handbook for Radiographers* , 13th ed., London: Hodder Arnold; 2010.

9. Davey E., England A. AP versus PA positioning in lumbar spine computed radiography: Image quality and individual organ doses. *Radiography* 2015;**21**(2):188–96. Doi: 10.1016/j.radi.2014.11.003.
10. Holm T., Palmer PES., Lehtinen E. *World Health Organization. Basic Radiological System: Manual of Radiographic Technique*, Geneva: World Health Organization; 1986.
11. Slosar P. Cervical Spine Anatomy. *Spine Health* . Available from: https://www.spine-health.com/conditions/spine-anatomy/cervical-spine-anatomy [accessed October 4, 2022].
12. Holmes K., Elkington M., Harris P. *Clark's Essential Physics In Imaging For Radiographers.* , Lancaster: University of Cumbria, School of Medical Imaging Sciences ; 2013.
13. Whitley S., Sloane C., Hoadley G., Moore A., Alsop C. *Clarke's Pocket Handbook for Radiographers*, 12th ed., London: Hodder Arnold; 2005.
14. UK Government. *The Ionising Radiation (Medical Exposure) Regulations 2017*, London: UK Statutory Instruments; 2017.
15. Landauer. ⅛" x ⅛" x 0.15" TLD-100H . *TLD Chip: Single Point Radiation Assessments*. Available from: https://www.landauer.co.uk/produit/tld-chip-single-point-radiation-assessments/ [accessed October 4, 2022].
16. J. Stratakis AP. Chapter 1 Dosimetry. *Radiation Dose Management of Pregnant Patients, Pregnant Staff and Paediatric Patients*, IOP Publishing; 2019.
17. Thermo Electron Corporation. *Thermo Fisher Scientific Harshaw TLD Model 5500 Reader with WinREMS Operator's Manual (5500-W-O-0805-006).* , 2005.
18. Hanna DW. *Development and optimization of a thermoluminescent dosimeter (TLD) analyser system for low-dose measurements utilizing photon counting techniques*. Kansas State University, Kansas , 1979.
19. International Commission on Radiological Protection. The 2007 Recommendations of the International Commission on Radiological Protection. *Annals of the ICRP* 2007;**103**.
20. European Guidelines on Quality Criteria for Diagnostic Radiographic Images. *European Guidelines on Quality Criteria for Diagnostic Radiographic Images*, 1996.
21. Hedberg EC., Ayers S. The power of a paired t-test with a covariate. *Soc Sci Res* 2015;**50**:277–91. Doi: 10.1016/j.ssresearch.2014.12.004.
22. The British Institute of Radiology. *Guidance on using shielding on patients for diagnostic radiology applications*, London; 2020.
23. Cancer Research UK. Risks and Causes of Thyroid Cancer. *Risks and Causes of Thyroid Cancer*. Available from: https://www.cancerresearchuk.org/about-cancer/thyroid-cancer/causes-risks [accessed October 4, 2022].
24. Robinson JB., Ali RM., Tootell AK., Hogg P. Does collimation affect patient dose in antero-posterior thoraco-lumbar spine? *Radiography* 2017;**23**(3):211–5. Doi: 10.1016/j.radi.2017.03.012.
25. Green C., Karnati G., Thomson K., Subramanian A. Lumbar spine radiographs — is it time for widespread adoption of posteroanterior projection? *Br J Radiol* 2019;**92**(1103):20190386. Doi: 10.1259/bjr.20190386.

26. Health and Care Professions Council. *Standards of Proficiency - Radiographers*, London; 2013.
27. Stephenson-Smith B., Neep MJ., Rowntree P. Digital radiography reject analysis of examinations with multiple rejects: an Australian emergency imaging department clinical audit. *J Med Radiat Sci* 2021;**68**(3):245–52. Doi: 10.1002/jmrs.468.
28. Don S., MacDougall R., Strauss K., Moore QT., Goske MJ., Cohen M., et al. Image Gently Campaign Back to Basics Initiative: Ten Steps to Help Manage Radiation Dose in Pediatric Digital Radiography. *American Journal of Roentgenology* 2013;**200**(5):W431–6. Doi: 10.2214/AJR.12.9895.
29. Singh T., Muscroft N., Collier N., England A. A comparison of effective dose and risk for different collimation options used in AP shoulder radiography. *Radiography* 2022;**28**(2):394–9. Doi: 10.1016/j.radi.2021.11.007.
30. Johnston J., Fauber TL. *Essentials of radiographic physics and imaging*, Elsevier Health Sciences; 2015.
31. National Institute for Health and Care Excellence. *Spinal injury: assessments and initial management*, London; 2016.
32. Head Injury: Assessment and Early Management. *National Institute for Health and Care* , London; 2021.
33. Loughman E., Rowan M., Kenny P. Does magnification increase total unsharpness in DR radiography? *Physica Medica* 2017;**42**:353. Doi: 10.1016/j.ejmp.2017.05.007.
34. Chaparian A., Kanani A., Baghbanian M. Reduction of radiation risks in patients undergoing some X-ray examinations by using optimal projections: A Monte Carlo program-based mathematical calculation. *J Med Phys* 2014;**39**(1):32. Doi: 10.4103/0971-6203.125500.
35. Bell D. Radiographic Distortion. *Radiopaedia*. Available from: https://radiopaedia.org/articles/radiographic-distortion?lang=gb [accessed October 4, 2022].
36. Nunn H. The Cervical Spine. *Image Interpretation* . Available from: https://www.imageinterpretation.co.uk/cervical.php [accessed October 4, 2022].